

A consistent model for both the HI and stellar mass functions of galaxies

Hazel Martindale^{1*}, Peter A. Thomas¹, Bruno M. Henriques^{2,3}, Jon Loveday¹

¹*Astronomy Centre, University of Sussex, Falmer, Brighton BN1 9QH, United Kingdom*

²*Max-Planck-Institut für Astrophysik, Karl-Schwarzschild-Str. 1, 85741 Garching b. München, Germany*

³*Institute for Astronomy, ETH Zurich, CH-8093 Zurich, Switzerland*

Submitted to MNRAS – 8 June 2021

ABSTRACT

Using the L-Galaxies semi-analytic model we simultaneously fit the HI mass function, stellar mass function and galaxy colours. We find good fits to all three observations at $z = 0$ and to the stellar mass function and galaxy colours at $z = 2$.

Using Markov Chain Monte Carlo (MCMC) techniques we adjust the L-Galaxies parameters to best fit the constraining data. In order to fit the HI mass function we must greatly reduce the gas surface density threshold for star formation, thus lowering the number of low HI mass galaxies. A simultaneous reduction in the star formation efficiency prevents the over production of stellar content. A *simplified* model in which the surface density threshold is eliminated altogether also provides a good fit to the data. Unfortunately, these changes weaken the fit to the Kennicutt-Schmidt relation and raise the star-formation rate density at recent times, suggesting that a change to the model is required to prevent accumulation of gas onto dwarf galaxies in the local universe.

Key words: methods: numerical – galaxies: formation – galaxies: evolution

1 INTRODUCTION

Cold gas provides the fuel for star formation and understanding its properties in galaxies is fundamental to a complete model of galaxy formation. While the physics governing the collapse of gas clouds on sub-pc scales, and its subsequent conversion into stars, remain largely unknown, simulations can be used to explore the factors that affect the gas and ultimately the stellar content of galaxies.

The relations governing star formation link the cold gas content to the amount of stars formed. The widely used Kennicutt-Schmidt relation (Schmidt 1959; Kennicutt 1998) is a relation between total cold gas content and the star formation rate of a galaxy. More recent observations, however, have shown the correlation to be stronger with only the molecular, H_2 component of cold gas (Bigiel et al. 2008; Leroy et al. 2008).

H_2 gas is not directly detected and is instead observed via the tracer molecule CO which adds uncertainty to these measurements. The HI component, on the other hand, correlates more weakly with star formation than the H_2 , but can be directly observed through the 21 cm emission. HI surveys such as the HI Parkes ALL-Sky Survey (HIPASS; Meyer et al. 2004) and the Arecibo Legacy Fast ALFA survey (ALFALFA; Giovanelli et al. 2005) now provide large samples of statistical significance. The HI mass function from these surveys measures masses down to $10^6 M_\odot$ allowing galaxy gas content to be probed across a full range of masses (Zwaan et al. 2005;

Martin et al. 2010). Up coming surveys at new facilities such as the Australian SKA pathfinder (ASKAP, Johnston et al. 2008), Karoo Array Telescope (MeerKAT, Booth et al. 2009) and the Square Kilometre Array (SKA¹) will greatly improve the observational constraints on HI content of galaxies. For that reason, we choose to use HI as a constraint in our models.

Semi-analytic models (SAMs) provide a framework to explore the statistical properties of the observed galaxy population. The evolution of large scale structures is given by dark matter merger trees, either from N-body simulations or analytic calculations, and the baryonic component is modelled via empirical relations that are designed to capture the key physics (White 1988; Cole 1991; Lacey & Silk 1991; White & Frenk 1991; Kauffmann, White & Guiderdoni 1993; Kauffmann 1999; Somerville & Primack 1999; Springel et al. 2001; Hatton et al. 2003; Kang et al. 2005; Croton et al. 2006; De Lucia & Blaizot 2007; Guo et al. 2011; Lu et al. 2011; Benson 2012). A downside of SAMs is that they necessarily impose restrictive assumptions about the geometry of galaxies and the exchange of material with their surroundings. The major advantage over hydrodynamical simulations is that they are quick to run allowing us to explore the impact of different implementations of physical processes and different parameter values. In recent years, the introduction of robust statistical methods has even allowed the full exploration of parameter space (Kampakoglou, Trotta & Silk 2008;

* E-mail: H.Martindale@sussex.ac.uk

¹ <https://www.skatelescope.org/project/>

Henriques et al. 2009; Benson & Bower 2010; Bower et al. 2010; Henriques & Thomas 2010; Lu et al. 2011, 2012; Mutch, Poole & Croton 2013; Henriques et al. 2013; Benson 2014; Ruiz et al. 2015).

The most recent version of the L-Galaxies SAM (Henriques et al. 2015, hereafter HWT15) provides an excellent fit to a wide range of galaxy properties across a wide range of redshifts. In this paper we aim to improve the agreement between the HWT15 model to the HI mass function by including it as an extra constraint in addition to the stellar mass function and galaxy colours. We find that we can obtain a good fit to all data-sets simultaneously by lowering, or even eliminating altogether, the surface density threshold for star formation. Unfortunately, these changes weaken the fit to the Kennicutt-Schmidt relation and raise the star-formation-rate density at recent times, suggesting that a change in the model is required to prevent accumulation of gas onto dwarf galaxies in the local Universe.

The paper is structured as follows: In Section 2 we describe the L-Galaxies semi-analytic model and the method of gas division. In Section 3 we present the results of constraining the model with the HI mass function in addition to the galaxy colours and stellar mass function. In Section 4 we examine which parameters have changed in order to produce a good fit to all constraining data sets and compare our results to the Kennicutt-Schmidt relation. We provide our conclusions in Section 5.

2 METHOD

2.1 L-Galaxies

Semi-analytic models provide a tool to explore galaxy formation and evolution and simulate the cosmic galaxy population. The models use coupled differential equations to follow the evolution of the baryonic component of galaxies usually constructed on top of dark matter halos from an N -body simulation. Many aspects of galaxy formation are included in these models such as, star formation, gas cooling, metal enrichment, black hole growth and feedback processes.

The Munich SAM, L-Galaxies, has been developed over many years using galaxy formation recipes to match the observed galaxy populations (White 1988; Kauffmann, White & Guiderdoni 1993; Kauffmann 1999; Springel et al. 2001, 2005; Croton et al. 2006; De Lucia & Blaizot 2007; Guo et al. 2011, 2013; Henriques et al. 2013; Henriques et al. 2015). The underlying merger trees are extracted from the Millennium (Springel et al. 2005) and MillenniumII Simulations (Boylan-Kolchin et al. 2009). The latest version of the model, on which this work is based, is given in HWT15. This version uses *Planck* year 1 cosmology with the Millennium dark matter merger trees scaled according to the method of Angulo & White (2010) (as updated by Angulo & Hilbert 2015). HWT15 constrain the model to give a good fit to the stellar mass function and the galaxy colours over the redshift range 0-3. A full description of the model is given in the supplementary material of HWT15.

2.1.1 MCMC

Having many recipes controlling galaxy formation gives rise to numerous free parameters which, when considering individual galaxy properties independently, are frequently degenerate with each other. It would be a long and inefficient process of trial and

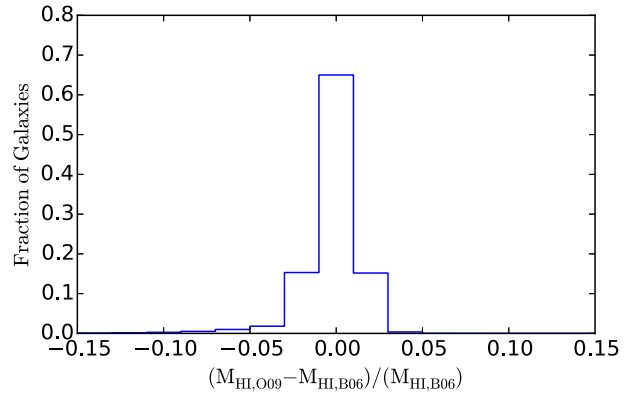


Figure 1. Histogram showing the difference between the HI mass calculated using BR06 and the approximation of O09.

error to adjust the parameters to best fit the observations by hand when alterations to the model are made. We employ the MCMC procedure within L-Galaxies to find a best fit set of parameters (Henriques et al. 2009; Henriques et al. 2013). This method approximates a likelihood value for the ability of the model to recover the observed galaxy property and then uses the MCMC technique to minimise that value and locate a best set of parameters.

2.1.2 Star formation law

In the model we assume stars form from the total cold gas within a given galaxy's disk (i.e. the model does not distinguish between HI and molecular gas). The star formation rate is given by

$$\dot{M}_{\text{stellar}} = \alpha_{\text{SF}} \frac{(M_{\text{gas}} - M_{\text{crit}})}{t_{\text{dyn,disk}}}, \quad (1)$$

where α_{SF} is a normalisation parameter, M_{gas} is the total cold gas mass, $t_{\text{dyn,disk}}$ is the dynamical time, and M_{crit} is a threshold mass whose need is based on a long-standing acceptance that there is a minimum surface density required for star formation (Kauffmann 1996; Kennicutt 1998). Based on the argument in Kauffmann (1996) we take M_{crit} to have the form

$$M_{\text{crit}} = M_{\text{crit},0} \left(\frac{V_{200c}}{200 \text{ km s}^{-1}} \right) \left(\frac{R_{\text{gas}}}{10 \text{ kpc}} \right), \quad (2)$$

where V_{200c} is the virial speed of the halo, R_{gas} is the gas disk scale-length, and $M_{\text{crit},0}$ is a normalisation constant. Since Kauffmann et al. (1999) and prior to HWT15, all versions of the Munich model fixed $M_{\text{crit},0} = 3.8 \times 10^9 M_{\odot}$. Recent work indicates that star formation is linked more closely to the molecular gas than to the total gas content (Bigiel et al. 2008; Leroy et al. 2008). This allows stars to form in regions with smaller total gas thresholds than previously and to allow for this we now (from HWT15 onwards) treat $M_{\text{crit},0}$ as a free parameter.

2.2 The HI model

We use the model of Blitz & Rosolowsky (2006, hereafter BR06) to divide the cold gas into its HI and H₂ components in post processing. In this model the ratio of HI to H₂ gas in a galaxy is determined by mid-plane hydrostatic pressure in the galactic disk. Elmegreen

(1989, 1993) propose a form for the mid-plane pressure

$$P_{\text{ext}} \approx \frac{\pi}{2} G \Sigma_{\text{gas}} \left(\Sigma_{\text{gas}} + \Sigma_{\text{star}} \frac{c_{\text{gas}}}{c_{\text{star}}} \right), \quad (3)$$

where Σ_{gas} , Σ_{star} are the cold gas and stellar surface densities, c_{gas} , c_{star} are the gas and stellar vertical velocity dispersions and G is the gravitational constant. The mid-plane pressure is calculated from the equations of hydrostatic equilibrium for a thin disk of gas and stars. This pressure is an important factor in the formation of giant clouds within which H_2 is found. BR06 make the assumption that the ratio of H_2 to H I in the galaxy is a function of the pressure given in (3). The relation takes the form of a power-law:

$$R_{\text{mol}} = \frac{\Sigma_{\text{H}_2}}{\Sigma_{\text{H I}}} = \left(\frac{P_{\text{ext}}}{P_0} \right)^\alpha \quad (4)$$

where Σ_{H_2} and $\Sigma_{\text{H I}}$ are the disk surface densities of H_2 and H I gas respectively and P_0 and α are fitting constants. This was further explored using resolved observations of galaxies (Blitz & Rosolowsky 2006; Leroy et al. 2008).

This model of gas division requires information on the radial distribution of gas inside galaxies. In order to include it at each step of the L-Galaxies MCMC chain without prohibitively slowing the calculation we use the approximation to BR06 model derived in Obreschkow et al. (2009, hereafter O09). They write R_{mol} as,

$$R_{\text{mol}} = R_{\text{mol}}^c \exp(-1.6 r/r_{\text{disk}}), \quad (5)$$

where r_{disk} is the scale length of the gas disk and R_{mol}^c is

$$R_{\text{mol}}^c = [K r_{\text{disk}}^{-4} M_{\text{gas}} (M_{\text{gas}} + \langle f_\sigma \rangle M_{\text{disk}}^{\text{stars}})]^\alpha, \quad (6)$$

where M_{gas} is the total cold gas mass, $M_{\text{disk}}^{\text{stars}}$ is the mass of the stellar disk and $K = G/(8\pi P_0)$. We adopt the same values of constants as O09: $P_0 = 2.34 \times 10^{-13} \text{ Pa}$, $\alpha = 0.8$ and $\langle f_\sigma \rangle = 0.4$. Through R_{mol} we can derive expressions for the surface density of H I and H_2 which when integrated give the $M_{\text{H I}}$ and M_{H_2} .

O09 approximate the integration, finding that the ratio of H_2 to H I is given by

$$\frac{M_{\text{H}_2}}{M_{\text{H I}}} = \frac{\int \Sigma_{\text{H}_2}(r) dA}{\int \Sigma_{\text{H I}}(r) dA} \approx (3.44 R_{\text{mol}}^{c-0.506} + 4.82 R_{\text{mol}}^{c-1.054})^{-1}. \quad (7)$$

Using this approximation along with assuming that $M_{\text{H}} = M_{\text{H I}} + M_{\text{H}_2}$ we can calculate the masses without dividing the galaxies into rings and significantly speed up the calculation. We assume that $M_{\text{H}} = 0.74 M_{\text{cold gas}}$. In Figure 1 we test the accuracy of this approximation for galaxies produced by our model. We show the difference in mass calculated using both approaches and find the agreement between the two methods to be excellent. We agree with the statement of O09 that the accuracy is greater than 5 per cent.

2.3 Observational Constraints

We constrain the model using observations at $z = 0$ and $z = 2$. At $z = 0$ we use:

- The stellar mass function is a combination of the SDSS (Li & White 2009) and GAMA (Baldry et al. 2012) results.
- The H I mass function is from HIPASS (Zwaan et al. 2005).
- The red fraction is obtained by dividing the stellar mass function of red galaxies by the sum of the red and blue stellar mass functions. We use data from Bell et al. (2003) and Baldry et al. (2012).

At $z = 2$:

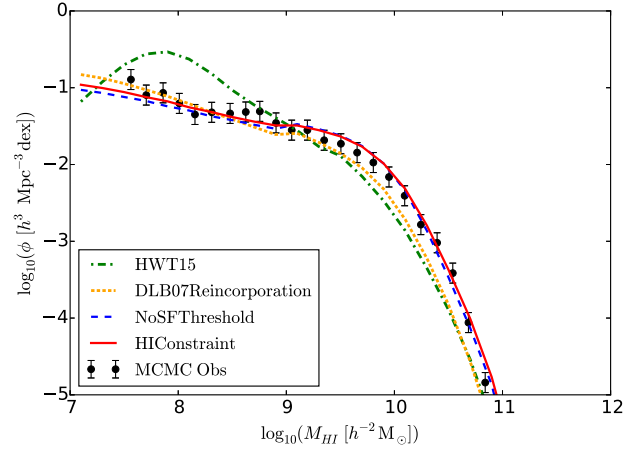


Figure 2. The H I mass function at $z=0$. The black points are the observed H I mass function from HIPASS. The coloured lines represent the different models: green, HWT15; red, HICConstraint; blue, NoSFThreshold; yellow, DLB07 Reincorporation.

- The stellar mass function is a combination of COSMOS (Domínguez Sánchez et al. 2011), ULTRAVISTA (Ilbert et al. 2013; Muzzin et al. 2013) and ZFOURGE (Tomczak et al. 2014).
- The red fraction of galaxies also uses COSMOS (Domínguez Sánchez et al. 2011), ULTRAVISTA (Ilbert et al. 2013; Muzzin et al. 2013) and ZFOURGE (Tomczak et al. 2014).

3 RESULTS

We present results for several different versions of the model:

- HWT15 (green dash-dotted line): The reference model, which did not use the H I MF as a constraint.
- HICConstraint (red solid line): The HWT15 model but adding in the H I MF as a constraint at $z = 0$.
- NoSFThreshold (blue dashed line): The same as the HICConstraint but with the minimum threshold surface density for star formation set equal to zero.
- DLB07Reincorporation (yellow dotted line): As for the HICConstraint but using the older (De Lucia & Blaizot 2007, hereafter DLB07) recipe for reincorporation of ejected material.

All of the the models were constrained to simultaneously match the observations described in Section 2.3, except HWT15 which did not use the H I MF as a constraint.

3.1 H I Mass Function

The H I mass function is shown in Figure 2. It is immediately obvious that the HWT15 reference model is a poor fit to observations. This is not an inherent deficiency of the model, but results from the fact that the observed mass function was not used as an input constraint. The HWT15 model does, in fact, provide a slightly better fit overall to the stellar masses and galaxy colours at $z = 0$ & 2, than the HICConstraint or NoSFThreshold model, but the difference is slight. That goes to show that the H I mass function serves as a largely independent constraint.

The HICConstraint model, however, that does use the H I as an additional constraint, provides a very good fit to the H I mass

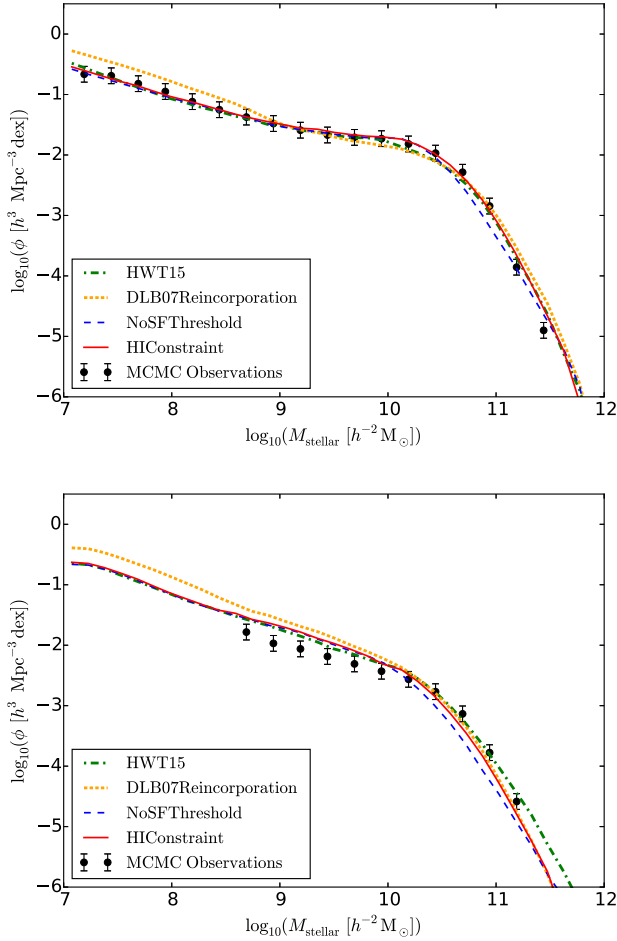


Figure 3. The stellar mass function, $z = 0$ is shown in the upper panel and $z = 2$ is shown in the bottom panel. The black points are the observations used within the MCMC as constraints. The coloured lines are as in Figure 2.

function. It does that largely by reducing the Σ_{SF} parameter in the model that governs the minimum surface density for quiescent star formation (see Table 1). This allows more cold gas to be consumed in low-mass galaxies. In order to maintain the same overall stellar mass, the star formation efficiency is reduced leading to a reduction of gas consumption in high-mass galaxies.

Because the HIConstraint model lowers the minimum surface density for star formation so much, we also examined a NoSFThreshold model in which it is set equal to zero (thus reducing the number of free parameters in the model by one). The two are barely distinguishable in their predictions (except that the NoSFThreshold model has slightly bluer colours – see Section 3.3).

To try to understand why Lu et al. (2014, hereafter Lu14) have claimed that it is not possible to reproduce the HI mass function, we also ran a model that is identical in every respect to the HIConstraint model, except that the reincorporation timescale follows the parameterisation given in DLB07 rather than HWT15. This DLB07 model, which uses HI as a constraint, provides a better fit than the original HWT15 but is clearly a significantly worse than either the HIConstraint or NoSFThreshold models. This will be discussed further in Section 4.3 below.

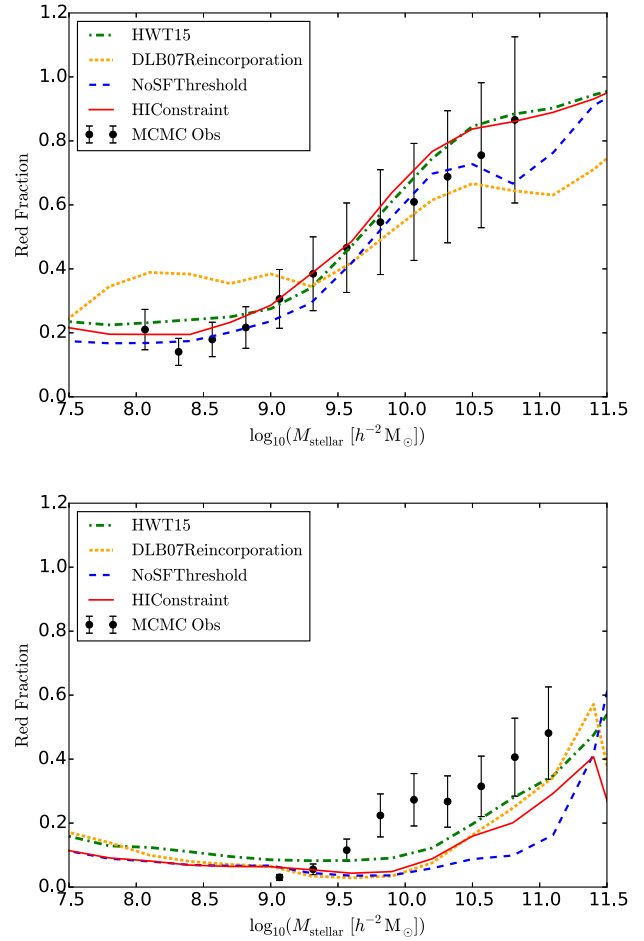


Figure 4. The red fraction mass function shown in the upper panel is $z = 0$ and $z = 2$ is shown in the lower. The line colours refer to the same models as those in Figure 3. The black points are the observed red fractions used with in the MCMC.

3.2 Stellar Mass Function

The stellar mass function is shown in Figure 3, the upper panel showing $z = 0$ and the lower $z = 2$. At $z = 0$ we find an excellent fit to the observed stellar mass function in both the HIConstraint and NoSFThreshold models, better even than that of the reference model of HWT15. There is no significant difference between the red and blue lines indicating that a non-zero threshold cold gas surface density is not required to fit the stellar mass function at $z = 0$. The DLB07 reincorporation model provides a significantly worse fit both at the knee of the SMF and the slope at low-masses. This is discussed further in Section 4.3.

The fit at $z = 2$ is a marginally worse than in HWT15 for both our models although the difference is very small. The DLB07 reincorporation model again fares worse than the others.

3.3 Galaxy Colours

The model was also constrained using the red fraction of galaxies, with the same prescription as HWT15. The red fraction is shown in Figure 4 with $z = 0$ in the upper panel and $z = 2$ in the lower panel. At $z = 0$ we have similar fits to HWT15, except for the

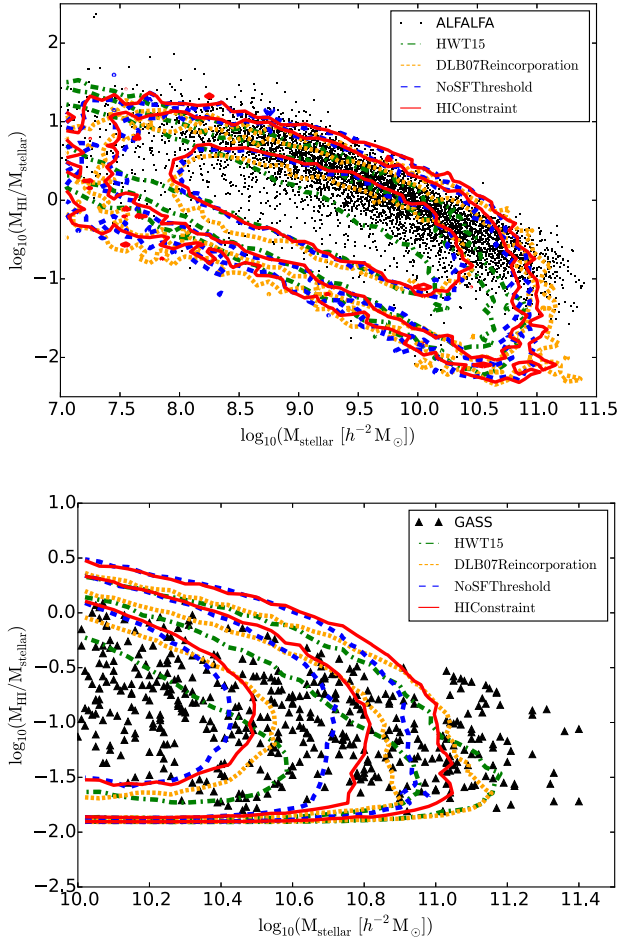


Figure 5. The HI to stellar mass fraction. Compare the HI mass to stellar mass fraction to observational data shown in black. The top panel compares our data to that from the ALFALFA survey, (Haynes et al. 2011). The lower panel compares with the GASS survey, triangles, (Catinella et al. 2013). We show each model as coloured contours. The dotted contour encloses 99 per cent of the data, the dashed contour encloses 95 per cent and the solid 68 per cent. For each survey we attempt to mimic the selection of each survey with the model data before comparing.

DLB07 model which has too few red galaxies at high masses and too many at low masses.

At $z = 2$ all models under predict the fraction of red galaxies at high stellar mass, with the NoSFThreshold model this time giving the poorest fit to the data. The decrease in the red population at $z = 2$ indicates the model has too much ongoing star formation in the highest mass galaxies. This suggests that the reduction of the threshold for star formation may not be an ideal solution to our problem, as discussed further in Section 4.2, below.

3.4 Gas Fractions

We calculate the H I to stellar mass ratio and compare to those observed by the ALFALFA, (Haynes et al. 2011), and GASS, (Catinella et al. 2013), surveys. In general we have good agreement with the observed H I gas fractions shown in Figure 5. The top panel of Figure 5 compares the models to ALFALFA while the bottom compares to GASS. The contour levels shown in Figure 5 for each model enclose 68, 90 and 99 per cent of the data. Our models galax-

ies reproduce the observations of the the GASS survey much more closely than those of ALFALFA.

The ALFALFA survey is a flux limited survey and due to limited sensitivity it can not observe very low H I mass galaxies. This leads to the survey missing low H I flux objects with correspondingly low gas fractions. In order to perform a detailed comparison we would need to precisely mimic the survey selection of ALFALFA in the model galaxies. In this work we perform a crude selection on the semi-analytic galaxies, converting the H I mass to a H I flux by setting an observer at the centre of the simulation box. We see from the top panel of Figure 5 that our model galaxies span the same range of stellar mass as the ALFALFA data and show the same upper limit in gas fraction (Maddox et al. 2015). However, the median ratio is offset significantly from that observed by ALFALFA. The comparison with an additional data set in the bottom panel suggests that this might result from the observational selection being more complex than the crude flux cut we have applied to the model galaxies. For example, there is also a dependence on the width of the observed spectral line.

In the lower panel of Figure 5 we compare our model results to the GASS survey. This should represent a more meaningful comparison since observations are stellar mass selected and have a much lower sensitivity to H I detection. Here, theoretical predictions match the observed gas fractions reasonably well.

In both the top and bottom panels of Figure 5 all 4 versions of the model are shown to produce similar results. The gas fractions is not currently a good measure to distinguish between the model versions. But, consistent with our findings on the mass functions, the original HWT15 model seems to have a lower H I mass fraction in high-mass galaxies than do the other models that use H I as a constraint.

4 DISCUSSION

4.1 Changes to model parameters

We start our discussion with the original HWT15 model and the new HICConstraint and NoSFThreshold models. We defer the discussion of the DLB07 model to the final paragraph of this section and Section 4.3.

The best fit parameters for our models are shown in Table 1. When adding in the H I mass function constraint into the HICConstraint and NoSFThreshold models several parameters have changed significantly from those of the original HWT15 model. The biggest change is to the surface density threshold for star formation, $M_{\text{crit},0}$, that we imposed. As described in Section 2.1.2 we have freed further the threshold parameter to allow it to become very low, or have forced its removal entirely, to allow a reduction in the H I content of low-mass galaxies. As compensation the star formation efficiency has decreased, preventing the over production of stars in more massive systems. The parameters controlling the feedback processes have changed slightly compared to HWT15. In Figure 6 we plot the formulae that control feedback as a function of virial velocity. These formulae can be found in the supplementary material of HWT15.

The top-left panel of Figure 6 shows that the new models prefer a sharp reduction in SN ejection efficiency above a halo circular speed of about 100 km s^{-1} , dropping to just 10-20 per cent at higher masses. This allows more retention of gas in high-mass systems. Slightly unexpectedly the mass-loading factors, shown in the top-right panel of the figure, are lower than for the fiducial HWT15

Parameter	HWT15	HiConstraint	NoSFThreshold	DLB07 Reincorporation	Units
α_{SF} (SF eff)	0.025	0.0081	0.012	0.0084	
Σ_{SF} (SF gas density threshold)	0.24	0.0018	1e-6	0.0024	$10^{10} M_{\odot} \text{pc}^{-2}$
$\alpha_{\text{SF,burst}}$ (SF Burst eff)	0.60	0.92	0.68	0.54	
$\beta_{\text{SF,burst}}$ (SF Burst Slope)	1.9	1.7	1.4	0.86	
k_{AGN} (Radio feedback eff)	0.0053	0.01	0.025	7.2×10^{-4}	$M_{\odot} \text{yr}^{-1}$
f_{BH} (Black hole growth eff)	0.041	0.042	0.022	0.030	
V_{BH} (Quasar growth scale)	750	900	840	300	km s^{-1}
ϵ (Mass-loading eff)	2.60	1.9	1.5	3.06	
V_{reheat} (Mass-loading scale)	480	270	370	100	km s^{-1}
β_1 (Mass-loading slope)	0.72	1.1	0.55	3.8	
η (SN ejection eff)	0.62	0.18	0.36	0.22	
V_{eject} (SN ejection scale)	100	200	120	150	km s^{-1}
β_2 (SN ejection Slope)	0.80	2.1	3.9	3.2	
γ (Ejecta reincorporation)	3.0×10^{10}	2.2×10^{10}	2.1×10^{10}	0.35	yr
y (Metal yield)	0.046	0.035	0.027	0.021	
R_{merger} (Major-merger threshold)	0.10	0.43	0.37	0.33	
α_{friction} (Dynamical friction)	2.5	4.5	4.3	2.5	
$M_{\text{r.p.}}$ (Ram-pressure threshold)	1.2×10^4	2.6×10^4	2.0×10^4	1.1	$10^{10} M_{\odot}$

Table 1. Parameters constrained by the MCMC model. Best fit parameters are given for each model as well as HWT15 for comparison.

model, except for DLB07Reincorporation that requires large mass-loading in dwarf galaxies to offset the rapid reincorporation (and subsequent cooling) of ejected gas (bottom-right panel). Unfortunately for that model, the expenditure of energy to heat extra cold gas results in a decrease of mass ejected in those dwarfs for a given amount of star-formation (lower-left panel); elsewhere that ratio is similar for all models over all masses.

Finally we identify a shift in the best fit value of the threshold between minor and major mergers with respect to the revised version of HWT15. That work found that there is some tension the value of this parameter required to match observations of the fraction of red galaxies and that required to match galaxy morphologies. HWT15 decided to fix R_{merge} at 0.1, slightly compromising colours at $z = 2$ to better match observed morphologies at $z = 0$. For the purposes of this paper, the main effect of a major merger is to destroy disks, turning HI gas into stars or reheating it into the hot phase. The threshold has increased from 0.1 in the HWT15 model to 0.33-0.43 in the new models. This sharp increase means many fewer mergers will be classed as major, allowing retention of more cold gas in massive galaxies. However, major mergers are also an important mechanism for creation of elliptical galaxies and the cessation of star formation. Their decrease contributes to the deficit of red galaxies we see in the lower panel of Figure 4.

4.2 Star formation

Figure 7 shows the effect that modifying our models has made to the Kennicutt-Schmidt relation. Both the observations and the model of HWT15 show a break in the power law relation at low surface densities which is not reproduced in the HiConstraint or NoSFThreshold models. The break arises naturally in the HWT15 from the finite threshold surface density for star formation. Although not imposed as a constraint it seems to arise through a need to prevent galaxies being too blue at $z = 2$. Once we include the HI mass function as a constraint, the break disappears because the improvement in that fit far outweighs the deterioration in the colours. We also see a shallower slope which is similar to

that observed between H_2 surface density and star formation rate (Bigiel et al. 2008; Wyder et al. 2009). This is perhaps an indicator that we should form stars only out of the H_2 component, although we show in Appendix A below that this does not, of itself, resolve the issues that we see here.

In Figure 8 we plot the star formation rate density (SFRD). All semi-analytic models tend to produce SFRDs that evolve too weakly at low redshift and L-Galaxies is no exception. At $z = 2$ all the models are very similar, while we start seeing more star formation in the new models at lower redshifts. By $z = 0$ there is significantly more star formation in the HiConstraint and NoSFThreshold models than in observations or HWT15. This is likely contributing to the deficit of red galaxies seen in Figure 4.

A more detailed gas division model such as that used in Fu et al. (2010, 2012) could solve the problems presented in this section. Fu et al. (2010, 2012) analysed the impact of different star formation and gas division recipes with spatially-resolved discs producing a match to the observed HI mass function (they still found an excess of dwarfs in the stellar mass function at $z = 2$, but this can likely be solved by the HWT15 gas reincorporation recipe). Spatially-resolved discs have not yet been implemented in the latest version of the Munich model. In order to try to understand the impact of these modifications in our work we have implemented a simplified version of the Fu model. This is described in Appendix A and goes some way to reconciling the Kennicutt-Schmidt relation with the HI mass function. There is therefore some indication that a more realistic gas division along with adjustments to the star formation relation may be the solution.

4.3 Comparison with other work

Lu14, who also use MCMC techniques to simultaneously fit the HI mass function and the K -band luminosity function, obtain much poor fits than we find and claim that generic deficiencies of current SAMS are: (i) extreme mass-loading factors are required in low-mass halos to expel the HI; (ii) the outflow requires more than

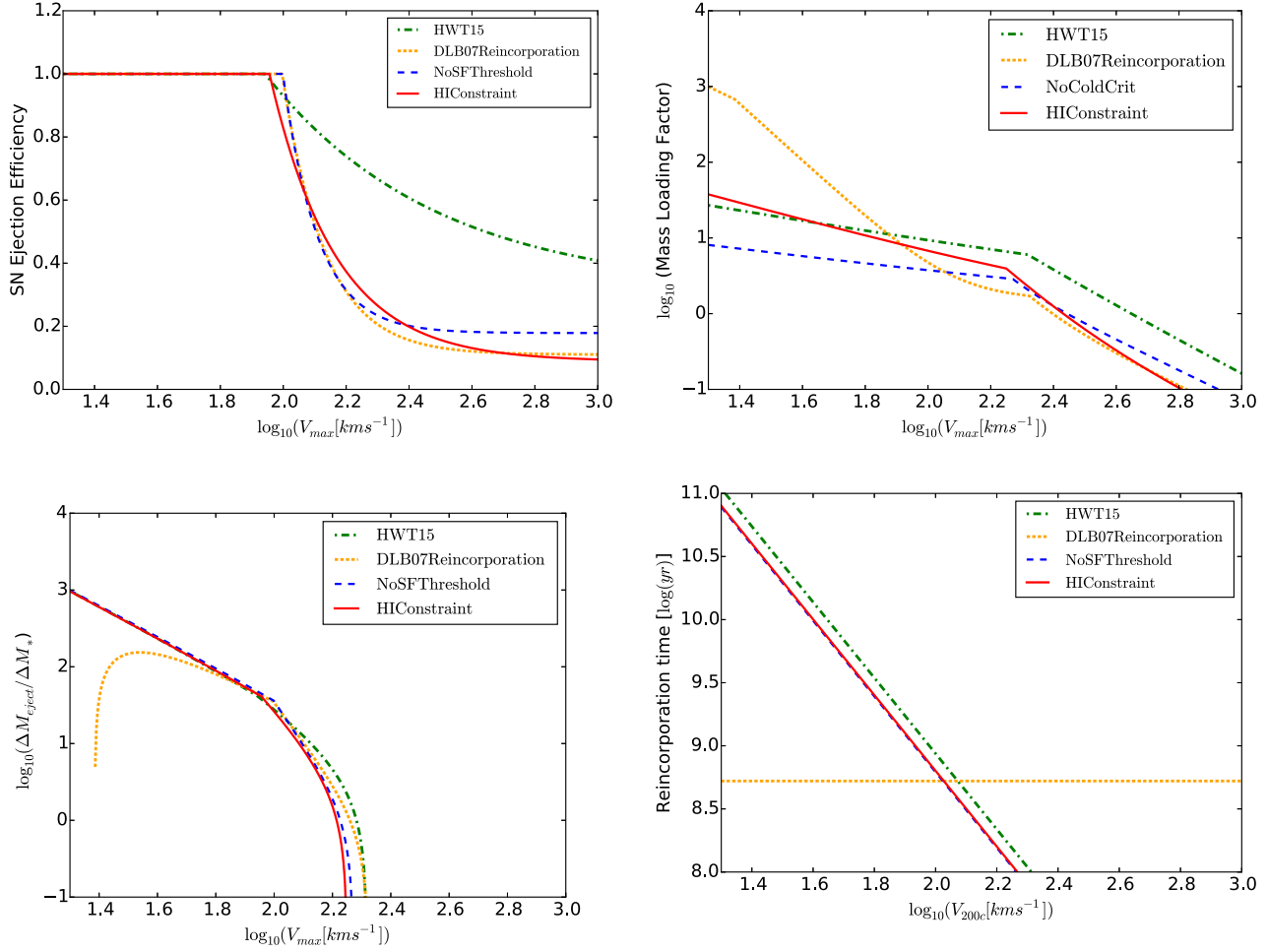


Figure 6. Supernova feedback parameters as functions of the halo velocity either maximum circular velocity, V_{max} or virial velocity V_{200c} . Top left is the SN Ejection Efficiency: the fraction of available SN energy for use in gas reheating and ejection. Top right is the Mass-loading Efficiency, that controls how much cold gas is reheated. Bottom left shows a derived quantity, the ratio of the mass of hot ejected gas to cold gas mass turned into stars. Finally, bottom right shows the Reincorporation Timescale for ejected gas. In all plots the colours represent the same models as described above. All plots are at $z = 0$.

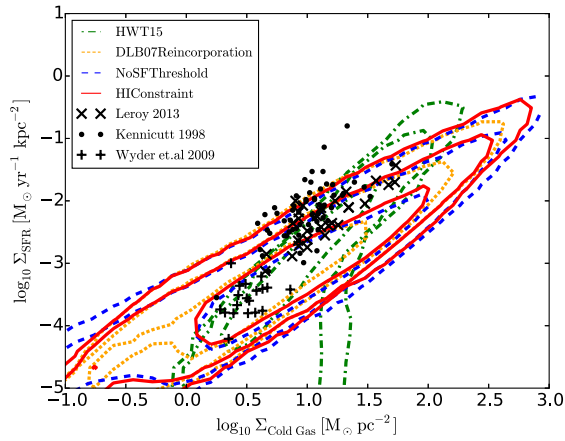


Figure 7. Relationship between total gas surface density and the star formation rate surface density. The contours again enclose 68, 95 and 99 per cent of the data. The colours represent the same 4 models as previously. The black data points represent observed values from three different studies (Kennicutt 1998; Leroy et al. 2013; Wyder et al. 2009).

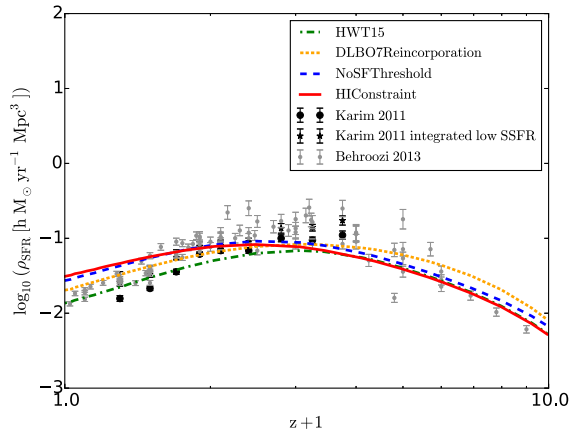


Figure 8. The cosmic star formation rate density. The colours again represent the 4 models. These are compared to observations with the black data points from Karim et al. (2011) and the grey from Behroozi, Wechsler & Conroy (2013).

25 per cent of the available supernova energy; and (iii) the star-formation histories of Milky-Way sized halos are far too flat.

We do not require extreme mass-loading factors to achieve the agreement with observations presented in this paper. As shown in Fig. S2 of HWT15, the values we assume are comparable to current observational estimates. On the other hand, we do require most of the supernova(SN) energy available to be used to power feedback. However, due to the uncertainties in the amount of energy produced by individual SN events we do not believe this rules out the models.

In an attempt to understand the differences in our findings we have undertaken a run using the reincorporation model of De Lucia & Blaizot (2007) which more closely matches that of Lu14. We do not get such a good fit to the HI mass function shown in Figure 2. As can be seen in the top left panel of Figure 6, with the DLB07 reincorporation recipe we find we require large mass loading factors in low mass galaxies and still don't get a good fit for the HI mass function. This could partially explain the differences between our results and those of Lu14.

Fu et al. (2010, 2012) integrate a model of gas division into a previous version of L-Galaxies, forming stars out of only the H_2 component without using MCMC to constrain the parameters. The model of gas division they use is more complex than that which we implement and the star formation recipe has no dependence on dynamical time. In addition, in regions where the molecular gas dominates the star formation goes as $\Sigma_{SF} \propto \Sigma_{H_2}$, while where atomic gas dominates $\Sigma_{SF} \propto \Sigma_{gas}^2$. Their work successfully reproduces the HI mass function. However, as discussed in Section 4.2 they do not reproduce the low mass end of the stellar mass function as well. Combining the work of Fu with HWT15 in future models of L-Galaxies could provide a solution to simultaneously producing the star forming properties and the HI mass function. This is hinted at in Appendix A.

Similar work has been undertaken in the Galform model by Lagos et al. (2011a,b) using the same pressure gas division model as used in this work. The gas division was included self consistently with stars being formed out of the H_2 component. They successfully reproduced the HI mass function but did not reproduce the stellar mass functions as well. Popping, Somerville & Trager (2014); Somerville, Popping & Trager (2015) also implement gas division in their semi-analytic model. They use several models of gas division and star formation and like Lagos et al. (2011a,b) they form stars from the H_2 component. They successfully reproduce several HI observations of galaxies. Their HI mass function exhibits a slight excess at low masses but fits well at the high mass end.

5 CONCLUSIONS

In this paper we have added the HI mass function as an observational constraint to the L-Galaxies semi-analytic model of Henriques et al. (2015). Using MCMC techniques we re-constrain the model parameters in order to best fit this extra observation at $z = 0$ in addition to the stellar mass function and galaxy colours at $z = 0$ and $z = 2$. The cold gas content of the model galaxies are divided in post processing into the HI and H_2 components using the gas division model of Blitz & Rosolowsky (2006) and the approximation to this from Obreschkow et al. (2009).

From this work we conclude :

(i) Using the $z = 0$ HI mass function as an extra constraint we obtain a good fit to this in addition to the stellar mass function and red fraction at $z = 0$ and $z = 2$.

(ii) The most important parameter change is the reduction of the star formation gas surface density threshold. This has been greatly reduced or even removed. This was required to remove the excess of HI gas seen in low mass galaxies in HWT15. As compensation, the star formation efficiency has decreased, preventing the over production of stars in more massive systems.

(iii) The feedback parameters have also changed. The retuned model favours a sharp reduction in the SN ejection efficiency above a halo circular speed of 100 km s^{-1} to much lower efficiencies compared to HWT15. The required mass loading factors are also reduced slightly compared to HWT15.

(iv) The model has a worse fit to the star formation properties shown in the Kennicutt-Schmidt relation and the cosmic star formation rate density at low redshifts. We see too much star formation $z = 0$, mostly in the low mass galaxies. This suggests that we either incorporate and cool too much gas, or that we underestimate the expulsion of gas via winds and stripping. However, since our red fractions roughly agree with observations, any changes must only reduce the star formation efficiency and not halt it completely.

(v) We use the reincorporation model of DLB07 to compare our model with that of Lu14. We alleviate some but not all of the problems identified by Lu14 through using an alternative reincorporation recipe. It is likely that a detailed model gas division and subsequent star formation will be required to match the observations.

Using a more detailed model of cold gas division and a change to the star formation recipe, such as those used in Fu et al. (2010, 2012, 2013), we expect to improve on the problems with simultaneously matching both the star formation properties and the observed HI mass function. In Appendix A we show a simplistic model in which we use the approximation for gas division given in Section 2.2 and then form stars only out of the molecular gas component. While the resulting HI mass function is not as good a fit as our HIConstraint model it is a significant improvement on the original HWT15 fit. Likewise for the Kennicutt-Schmidt relation the model shown in Appendix A is an improvement on the HIConstraint model shown in Figure 7.

In summary, the cold gas mass function provides a useful constraint on galaxy formation models that poses challenges to the current paradigm. It is difficult to lower the HI mass function in low-mass galaxies without violating the Kennicutt-Schmidt star formation law and having too much star-formation in dwarf galaxies in the current-day Universe. It is likely that a detailed model of the cold gas in the HI and H_2 components and subsequent star formation is required to resolve the issue.

ACKNOWLEDGEMENTS

All authors contributed to the development of the model, the interpretation of the results, and the writing of the paper. HM led the bulk of the data analysis and wrote the initial draft the paper.

The analysis was undertaken on the APOLLO cluster at Sussex. This research made use of Astropy, a community-developed core Python package for Astronomy (Robitaille et al. 2013). HM(ORCID 0000-0001-6953-7760) acknowledges the support of her PhD studentship from the Science and Technology Facilities Council (ST/K502364/1). PAT(ORCID 0000-0001-6888-6483) and JL acknowledge support from the Science and Technology Facilities Council (grant number ST/L000652/1). The work of BH(ORCID 0000-0002-1392-489X) was supported by Advanced Grant 246797 "GALFORMOD" from the European Research Council and by a Zwicky Fellowship.

REFERENCES

- Angulo R. E., Hilbert S., 2015, *MNRAS*, 448, 364
- Angulo R. E., White S. D. M., 2010, *MNRAS*, 405, 143
- Baldry I. K. et al., 2012, *Mon. Not. R. Astron. Soc.*, 421, no
- Behroozi P. S., Wechsler R. H., Conroy C., 2013, *Astrophys. J.*, 770, 57
- Bell E. F., McIntosh D. H., Katz N., Weinberg M. D., 2003, *Astrophys. J. Suppl. Ser.*, 149, 289
- Benson A. J., 2012, *New Astron.*, 17, 175
- Benson A. J., 2014, *Mon. Not. R. Astron. Soc.*, 444, 2599
- Benson A. J., Bower R., 2010, *Mon. Not. R. Astron. Soc.*, 405, no
- Bigiel F., Leroy A., Walter F., Brinks E., de Blok W. J. G., Madore B., Thornley M. D., 2008, *Astron. J.*, 136, 2846
- Blitz L., Rosolowsky E., 2006, *Astrophys. J.*, 650, 933
- Booth Ê., deÊBlok Ê., Jonas Ê., Fanaroff Ê., 2009, eprint arXiv:0910.2935
- Bower R. G., Vernon I., Goldstein M., Benson A. J., Lacey C. G., Baugh C. M., Cole S., Frenk C. S., 2010, *Mon. Not. R. Astron. Soc.*, 407, 2017
- Boylan-Kolchin M., Springel V., White S. D. M., Jenkins A., Lemson G., 2009, *Mon. Not. R. Astron. Soc.*, 398, 1150
- Catinella B. et al., 2013, *Mon. Not. R. Astron. Soc.*, 436, 34
- Cole S., 1991, *Astrophys. J.*, 367, 45
- Croton D. J. et al., 2006, *Mon. Not. R. Astron. Soc.*, 365, 11
- De Lucia G., Blaizot J., 2007, *Mon. Not. R. Astron. Soc.*, 375, 2
- Domínguez Sánchez H. et al., 2011, *Mon. Not. R. Astron. Soc.*, 417, 900
- Elmegreen B. G., 1989, *Astrophys. J.*, 338, 178
- Elmegreen B. G., 1993, *Astrophys. J.*, 411, 170
- Fu J., Guo Q., Kauffmann G., Krumholz M. R., 2010, *Mon. Not. R. Astron. Soc.*, 409, 515
- Fu J. et al., 2013, *Mon. Not. R. Astron. Soc.*, 434, 16
- Fu J., Kauffmann G., Li C., Guo Q., 2012, *Mon. Not. R. Astron. Soc.*, 424, 2701
- Giovanelli R. et al., 2005, *Astron. J.*, 130, 2598
- Guo Q., White S., Angulo R. E., Henriques B., Lemson G., Boylan-Kolchin M., Thomas P., Short C., 2013, *Mon. Not. R. Astron. Soc.*, 428, 1351
- Guo Q. et al., 2011, *Mon. Not. R. Astron. Soc.*, 413, 101
- Hatton S., Devriendt J. E. G., Ninin S., Bouchet F. R., Guiderdoni B., Vibert D., 2003, *Mon. Not. R. Astron. Soc.*, 343, 75
- Haynes M. P. et al., 2011, *Astron. J.*, 142, 170
- Henriques B. M. B., Thomas P. A., 2010, *Mon. Not. R. Astron. Soc.*, 403, 768
- Henriques B. M. B., Thomas P. A., Oliver S., Roseboom I., 2009, *Mon. Not. R. Astron. Soc.*, 396, 535
- Henriques B. M. B., White S. D. M., Thomas P. a., Angulo R., Guo Q., Lemson G., Springel V., Overzier R., 2015, *Mon. Not. R. Astron. Soc.*, 451, 2663
- Henriques B. M. B., White S. D. M., Thomas P. A., Angulo R. E., Guo Q., Lemson G., Springel V., 2013, *MNRAS*, 431, 3373
- Ilbert O. et al., 2013, *Astron. Astrophys.*, 556, A55
- Johnston S. et al., 2008, *Exp. Astron.*, 22, 151
- Kampakoglou M., Trotta R., Silk J., 2008, *Mon. Not. R. Astron. Soc.*, 384, 1414
- Kang X., Jing Y. P., Mo H. J., Borner G., 2005, *Astrophys. J.*, 631, 21
- Karim A. et al., 2011, *Astrophys. J.*, 730, 61
- Kauffmann G., 1996, *Mon. Not. R. Astron. Soc.*, 281
- Kauffmann G., 1999, *Am. Astron. Soc. Meet. Abstr.*, 195
- Kauffmann G., White S. D. M., Guiderdoni B., 1993, *Mon. Not. R. Astron. Soc.*, 264, 201
- Kennicutt R. C., 1998, *Astrophys. J.*, 498, 541
- Lacey C., Silk J., 1991, *Astrophys. J.*, 381, 14
- Lagos C. d. P., Baugh C. M., Lacey C. G., Benson A. J., Kim H.-S., Power C., 2011a, *Mon. Not. R. Astron. Soc.*, 418, 1649
- Lagos C. d. P., Lacey C. G., Baugh C. M., Bower R. G., Benson A. J., 2011b, *Mon. Not. R. Astron. Soc.*, 416, 1566
- Leroy A. K., Walter F., Brinks E., Bigiel F., de Blok W. J. G., Madore B., Thornley M. D., 2008, *Astron. J.*, 136, 2782
- Leroy A. K. et al., 2013, *Astron. J.*, 146, 19
- Li C., White S. D. M., 2009, *Mon. Not. R. Astron. Soc.*, 398, 12
- Lu Y., Mo H. J., Katz N., Weinberg M. D., 2012, *Mon. Not. R. Astron. Soc.*, 421, 1779
- Lu Y., Mo H. J., Lu Z., Katz N., Weinberg M. D., 2014, *Mon. Not. R. Astron. Soc.*, 443, 1252
- Lu Y., Mo H. J., Weinberg M. D., Katz N., 2011, *Mon. Not. R. Astron. Soc.*, 416, 1949
- Maddox N., Hess K. M., Obreschkow D., Jarvis M. J., Blyth S.-L., 2015, *Mon. Not. R. Astron. Soc.*, 447, 1610
- Martin A. M., Papastergis E., Giovanelli R., Haynes M. P., Springob, Christopher M. Stierwalt S., 2010, *Astrophys. J.*, 723, 1359
- Meyer M. J. et al., 2004, *Mon. Not. R. Astron. Soc.*, 350, 1195
- Mutch S. J., Poole G. B., Croton D. J., 2013, *Mon. Not. R. Astron. Soc.*, 428, 2001
- Muzzin A. et al., 2013, *Astrophys. J.*, 777, 18
- Obreschkow D., Croton D., De Lucia G., Khochfar S., Rawlings S., 2009, *Astrophys. J.*, 698, 1467
- Popping G., Somerville R. S., Trager S. C., 2014, *Mon. Not. R. Astron. Soc.*, 442, 2398
- Robitaille T. P. et al., 2013, *Astron. Astrophys.*, 558, A33
- Ruiz A. N. et al., 2015, *Astrophys. J.*, 801, 139
- Schmidt M., 1959, *Astrophys. J.*, 129, 243
- Somerville R. S., Popping G., Trager S. C., 2015, *Mon. Not. R. Astron. Soc.*, 453, 4338
- Somerville R. S., Primack J. R., 1999, *Mon. Not. R. Astron. Soc.*, 310, 1087
- Springel V. et al., 2005, *Nature*, 435, 629
- Springel V., White S. D. M., Tormen G., Kauffmann G., 2001, *Mon. Not. R. Astron. Soc.*, 328, 726
- Tomczak A. R. et al., 2014, *ApJ*, 783, 85
- White S. D. M., 1988, *NATO Adv. Sci. Institutes Ser. C*, 264
- White S. D. M., Frenk C. S., 1991, *Astrophys. J.*, 379, 52
- Wyder T. K. et al., 2009, *Astrophys. J.*, 696, 1834
- Zwaan M. A., Meyer M. J., Staveley-Smith L., Webster R. L., 2005, *Mon. Not. R. Astron. Soc. Lett.*, 359, L30

APPENDIX A: STAR FORMATION FROM MOLECULAR GAS

We have investigated the effect of using the approximation given in Equation 7 in order to form stars out of only the H₂ component of the cold gas. We modify Equation 1 so that the gas mass is that of just the H₂ component and there is no longer any gas density threshold. The resulting H I mass function and Kennicutt-Schmidt relation are shown in Figure A1 and Figure A2, respectively. In the H I mass function we see a slight excess of galaxies with low H I masses, significantly better than the original HWT15 but slightly worse than our best fit H IConstraint model. The new model roughly fits the slope of KS relation, although it might not have a sharp enough break at low masses. We conclude that the formation of stars out

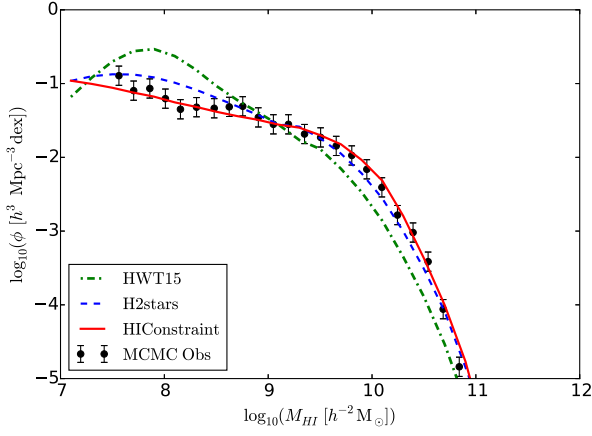


Figure A1. The H I mass function. The red and green lines are as in previous figures; the blue line uses the gas division approximation to form stars out of only H₂ gas.

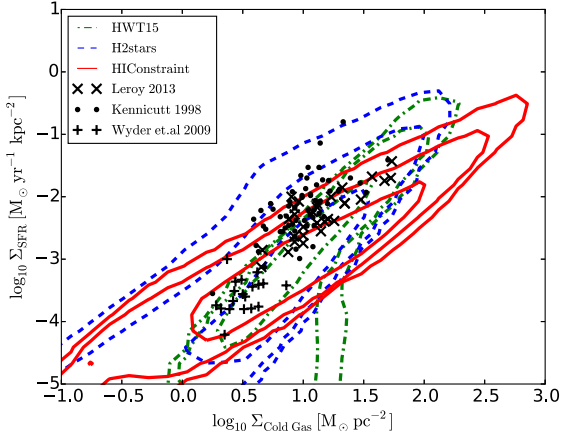


Figure A2. Relationship between total gas surface density and the star formation rate. The contours again enclose 68, 95 and 99 per cent of the data. The red and green are as in previous figures and the blue uses the gas division approximation to form stars out of only H₂ gas. The black data points represent observed values from three different studies (Kennicutt 1998; Leroy et al. 2013; Wyder et al. 2009).

of only the H₂ component gives an interesting compromising in the comparison between model and observations for the H I mass function and KS relation. A detailed model of H₂ conversion and subsequent star formation might correct the excessive cold gas in the lowest mass galaxies.